Response to the comments of Referee #2

Dear Reviewer,

We sincerely thank the reviewers for the thorough and constructive comments, which have substantially improved the manuscript. We have carefully addressed all comments point by point below. In this response letter, our replies to each comment are presented in blue text, and revised manuscript text is highlighted in yellow. All changes are indicated in the revised manuscript using tracked changes.

....

This study presents a case study for refractory black carbon (rBC) coating thickness evolution with different chemical compositions based on airborne measurements during winter 2025. Coating thickness fraction of rBC during a stagnant event is discussed and its correlation with different species is evaluated.

Overall, this manuscript applies reasonable evaluation. However, the interpretation of rBC mode diameter is confusing, and the size bins for rBC coating sensitivity tests remain questionable. Back trajectory analysis is recommended to characterize air mass history, rather than relying on wind direction alone. The manuscript requires thorough editing before it can be considered for publication.

Major:

1. Figure 1 and table 1, most samples were collected within the boundary layer, and trace gases and aerosols exhibited strong altitude dependence. The discussion should therefore exclude the ascending and descending profiles and focus solely on boundary layer conditions, with the vertical profiles (Figure 2) addressed separately.

We thank the reviewer for this insightful suggestion. We agree that distinguishing vertical *transitions from level flights is critical for a clear evaluation of boundary layer characteristics versus vertical structure.*

We would like to clarify that in the original manuscript, the statistics presented in Tables 1 and 2 were already calculated using only data collected within the boundary layer. Because direct in situ marine boundary layer height measurements were unavailable, we utilized the planetary boundary layer height (PBLH) derived from ECMWF ERA5 reanalysis data at the nearest grid points to define the boundary layer top for each flight (details provided in Sect. S2 of the Supplement).

Furthermore, to improve clarity, Figure 2 has been revised to explicitly distinguish between ascending/descending profiles (open circles) and level flight segments (colored circles), allowing the reader to clearly identify data collected under steady boundary layer sampling conditions versus vertical transition periods.

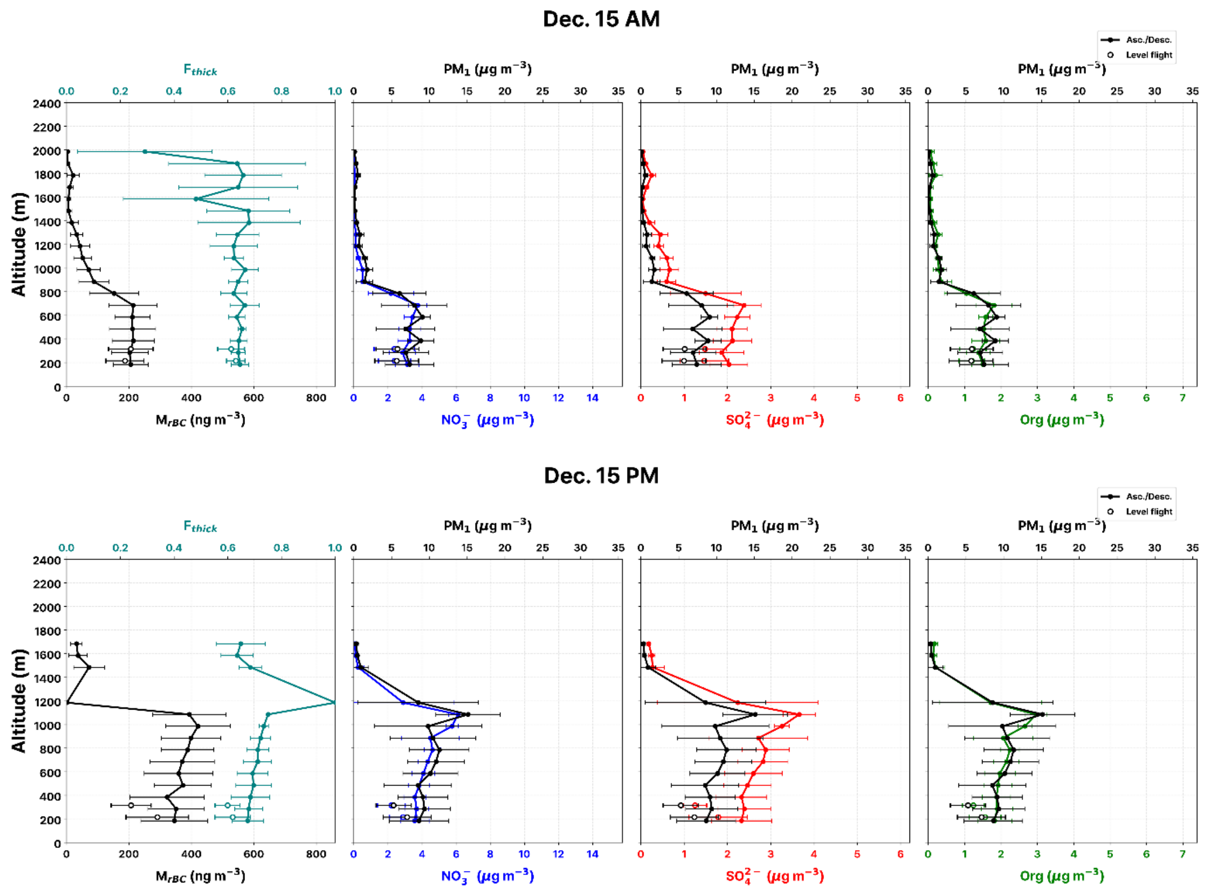

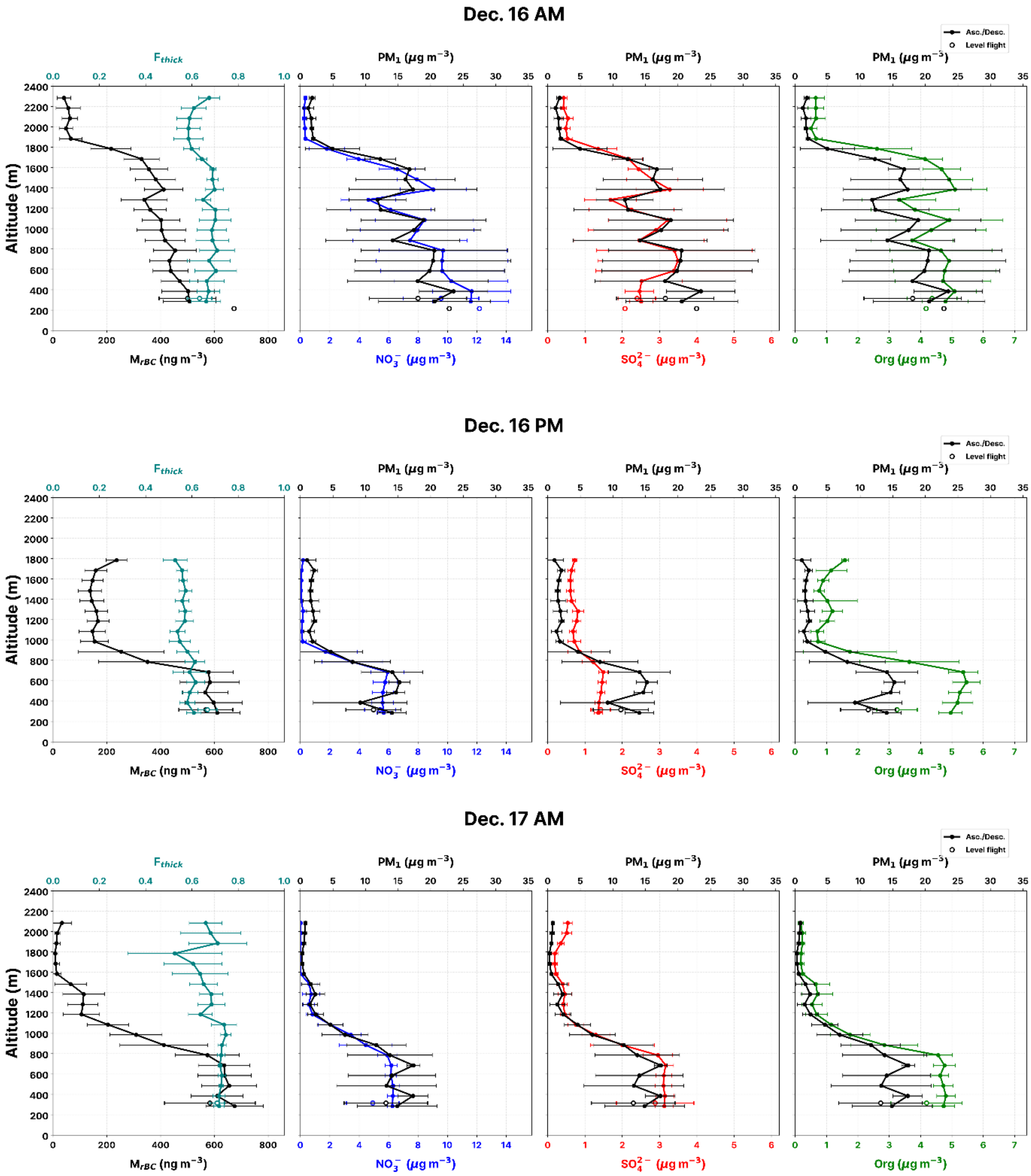
Dec. 16 AM
Dec. 16 PM
Dec. 17 AM
Asc./Desc.
Level flight
F_thick
PM1 (μg m−3)
Altitude (m)
M_rBC (ng m−3)
NO3− (μg m−3)
SO42− (μg m−3)
Org (μg m−3)

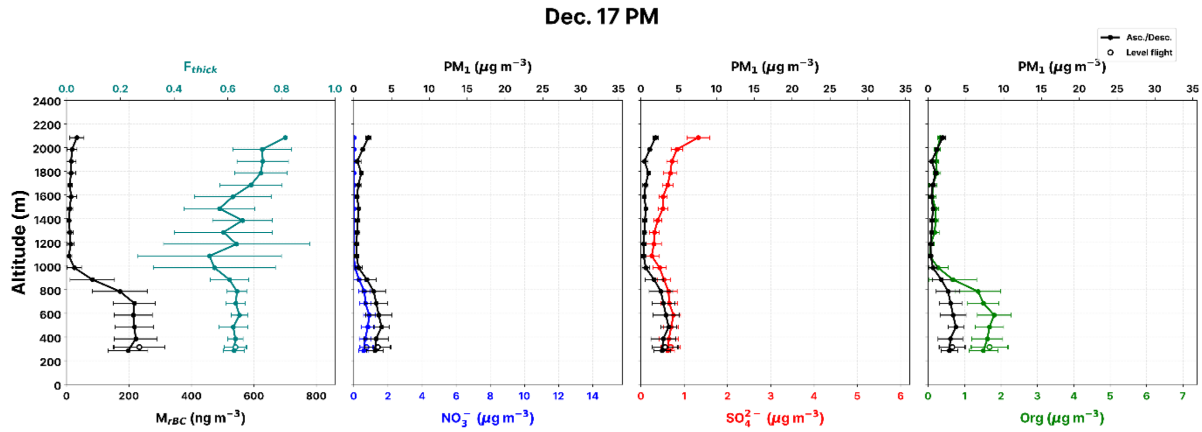

Figure 2. Research flight-wise vertical profiles of rBC properties (M_{rBC} and F_{thick}) and NR-PM_1 species concentrations observed during the intensive periods: (a) Dec. 15 AM; (b) Dec. 15 PM; (c) Dec. 16 AM; (d) Dec. 16 PM; (e) Dec. 17 AM; and (f) Dec. 17 PM. Open circles denote data collected during ascending and descending profiles, while filled colored circles represent level flight segments. The data points and error bars represent the mean and standard deviation of 1-s (1-m for F_{thick}) measurements aggregated into 100-m altitude bins. Wider F_{thick} error bars above ~1,600 m (panels a, f) result from reduced rBC number counts aloft. Statistical significance of the vertical gradients across altitude bins was evaluated using Kruskal–Wallis *H* tests for each flight session (Table S1).

2. Line 210-211, in section 2, the rBC mass median diameter was defined by a log-normal distribution, then it should not have a mode 1 but one value. The description is confusing throughout. It mentioned mode 2 in later subsections, but the figure 1 only showed one line. In RF1, the bimodal distribution has a mode 1 as ~151 nm. A 1-nm difference between RF1 and RF2 is trivial.

We thank the reviewer for this careful reading. We agree that the description was inconsistent and potentially confusing. Since the rBC core size distribution was characterized *by a single log-normal fit yielding one mass median diameter (MMD) per flight, references to "mode 1" and "mode 2" have been removed throughout the manuscript. All size distribution descriptions now refer solely to the MMD derived from the log-normal fit, consistent with Figure 1 and the methodology described in Sect. 2.2.*

The F_{thick} changed from 0.62±0.04 to 0.63±0.06 doesn't seem statistics significant, which does not mean a subtle increase.

We acknowledge that the flight-to-flight differences in mean F_{thick} are individually small (within ~10% across the full event), yet the progressive increase in mean F_{thick} from RF1 (0.62) through RF5 (0.70) coincides consistently with a parallel rise in the BZ/TOL ratio (Tabl1 1 and Figure 3), suggesting a physically coherent temporal trend in rBC aging rather than random variability.

Furthermore, to contextualize the interpretive significance of such changes, we draw on compiled F_{thick} observations across diverse Asian environments. Please find the figure below, which is adapted from a recent publication from our research group (Mishra et al., 2026). As comprehensively compiled across diverse Asian environments in this work, ambient F_{thick} exhibits a characteristic dynamic baseline dictated by site classification and aging state. In the figure abovementioned, some urban sites (e.g., Seoul, Xianyang, Xiamen) include lower F_{thick} baselines (~20-40%), whereas regional background sites (e.g., Noto Peninsula, Lijiang) consistently maintain higher baselines around ~70-80%.

Crucially, within a specific region, the baseline variability (indicated by standard deviations or error bars) is characteristically constrained. Individual regional background sites exhibit narrow variability (error bars within ~5%), such as Noto Peninsula and Lijiang. In contrast, the Yellow Sea airborne dataset exhibits a noticeably larger standard deviation, ~20 %. This *broader variability stems directly from the various flight altitude ranges and the multi-year observation span encompassing diverse seasonal transitions, contrasting synoptic regimes, and varying degrees of plume aging across multiple transboundary episodes.*

In another study investigating F_{thick} in an urban atmosphere during a single winter period (a month), F_{thick} increased tightly with $PM_{2.5}$, with its mean ~50% to 63% in $PM_{2.5}$ each bin (Figure R2, Lim et al., 2025).

These observational data of F_{thick} demonstrates that within a single targeted winter haze episode (3 days), baseline variability remains tightly constrained. Consequently, in this study, an absolute shift in F_{thick} reflects a physically meaningful transition in the rBC mixing state rather than instrumental noise.

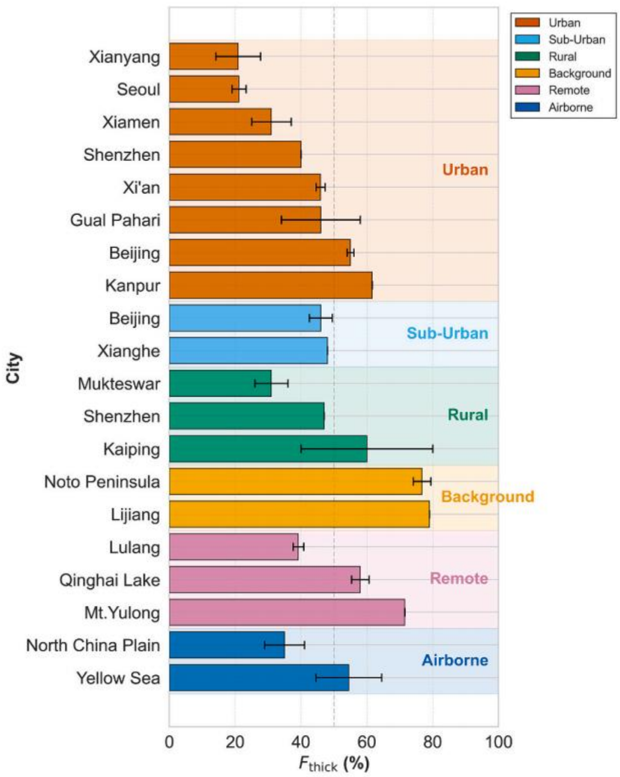

Fig. 7. F_{thick} (Number fraction of Thickly coated particles) of BC in different site types. The values shown are the average and standard deviation (shown with error bars) of all the reported values in a region that has been identified under a specific site category.

Figure R1. F_{thick} of BC in different site types (source: Mishra et al., 2026).

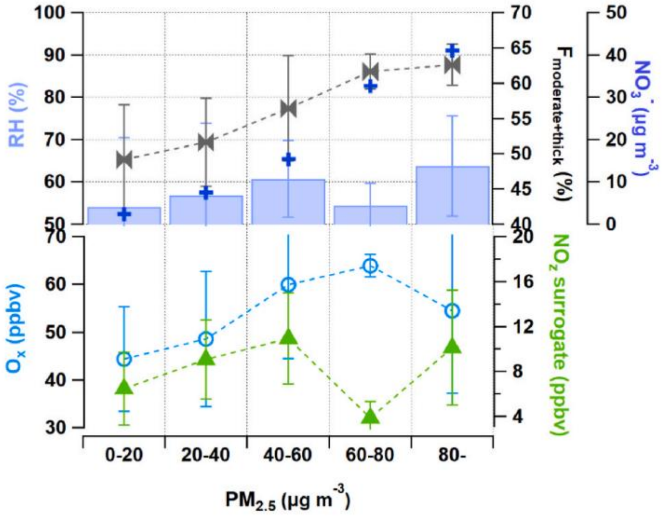

Figure R2. Variations of $F_{moderate+thick}$ and other measurement parameters as a function of $PM_{2.5}$ at urban Seoul in October to November of the 2021. Adapted from Lim et al. (2025). $F_{moderate+thick}$ is identical to F_{thick} in this study.

We added this statement, incorporating the references, Mishra et al. (2026) and Lim et al. (2025) in Section 2.2.

L159: It is noteworthy that the variability of F_{thick} (e.g., standard deviation) was often within ~10% at single observation sites in both urban and well-aged background environments (Lim et al., 2025; Shalini et al., 2026). Within a given region and season, baseline fluctuations are tightly bounded; thus, an absolute shift of ~10% or less is not statistically trivial, but marks a meaningful transition in the BC mixing state.

In addition, in figure 2, to directly address whether the vertical variability of F_{thick} across

100-m altitude bins reflects genuine physical gradients rather than observational noise, we performed non-parametric Kruskal–Wallis H tests across the vertical bins for each individual flight session.

As summarized in the test results below, the vertical gradients of F_{thick} are statistically significant across most flight periods. The weaker statistical significance on 16 Dec. AM ($p < 0.05$) and the lack of significance on 16 Dec. PM are attributable to distinct meteorological and aerosol dispersion conditions. Under relatively stagnant atmospheric condition, NR-PM_1 concentrations were elevated up to 1.8 km a.s.l. on 16 Dec. AM, while high aerosol loadings remained trapped within the boundary layer during the afternoon, resulting in F_{thick} being uniformly distributed. Thus, the absence of sharp vertical differences on 16 Dec. accurately captures a well-mixed, persistent haze layer rather than instrumental insensitivity. In addition, the comparatively moderate statistical significance on 17 Dec. PM ($p<0.05$*) is physically and observationally consistent with the vertical profile (Figure 2f). Within the lower boundary layer (below ~900 m a.s.l.), all aerosol constituents and F_{thick} were vertically well-mixed and uniform, while sparse particle counts in the clean air aloft substantially broadened the F_{thick} uncertainty, inflating the overall p value rather than reflecting measurement ambiguity.*

We have added these Kruskal–Wallis test results to the Supplementary Information (Table S1) and clarified statistical test done in Figure 2 caption.

Table S1. Kruskal–Wallis test of vertical F_{thick} variability across 100-m altitude bins for each flight session.

Flight	Total Samples (N)	P value
Dec. 15 AM	157	<0.0001***
Dec. 15 PM	152	<0.0001***
Dec. 16 AM	161	<0.05*

Dec. 16 PM	112	Not significant
Dec. 17 AM	131	<0.01**
Dec. 17 PM	121	<0.05*

Figure 2. Research flight-wise vertical profiles of rBC properties (M_{rBC} and F_{thick}) and NR-PM_1 species concentrations observed during the intensive periods: (a) Dec. 15 AM; (b) Dec. 15 PM; (c) Dec. 16 AM; (d) Dec. 16 PM; (e) Dec. 17 AM; and (f) Dec. 17 PM. Open circles denote data collected during ascending and descending profiles, while filled colored circles represent level flight segments. The data points and error bars represent the mean and standard deviation of 1-s (1-m for F_{thick}) measurements aggregated into 100-m altitude bins. Wider F_{thick} error bars above ~1,600 m (panels a, f) result from reduced rBC number counts aloft. Statistical significance of the vertical gradients across altitude bins was evaluated using Kruskal–Wallis *H* tests for each flight session (Table S1).

3. Figure 1 and Line 213-216, there are two distinct CO/CO_2 ratios on RF2, one before 2:50pm, and one after. Since there are no flight trajectories, it is hard to justify whether this is an increase compared to RF1, or just a spatial variation.

We thank the reviewer for this careful observation. We agree that without flight trajectory information, it is difficult to distinguish temporal evolution from spatial variability. As now shown in the added flight track figure (Figure S1), both Dec. 15 AM and Dec. 15 PM flights operated along an identical spatial corridor originating from Anmyeon-do, transiting west-northwest over the Yellow Sea, and returning along the same track (Figure R3). The only spatial deviation during Dec. 15 PM was a vertical sounding maneuver near 36.6°N, 124.2°E at approximately 14:50 KST, before and after which the horizontal flight path was identical to *the AM flight.*

Regarding the two distinct CO/CO_2 ratio regimes within RF2: the pre-14:50 KST level leg already showed systematically elevated CO and rBC concentrations compared to the AM flight over the same geographic coordinates, indicating that the shift reflects an air mass change over time rather than a spatial artifact. In-boundary-layer averages show consistent regional increases from AM to PM for CO (from 0.18±0.07 ppmv to 0.23±0.09 ppmv), CO2 (from 442.9±3.0 ppmv to 446.3±3.6 ppmv), and MrBC (from 185.8±64.3 ng m^{-3} to 280.4±92.8 ng m^{-3}). We therefore attribute the AM-to-PM differences to the initial regional arrival of continental outflow over the Yellow Sea, rather than to flight path discrepancies. The intra-flight CO/CO_2 variability within RF2 likely reflects the temporal progression of this arriving plume during the sampling period, and we have revised the manuscript text to reflect this interpretation with appropriate caution.

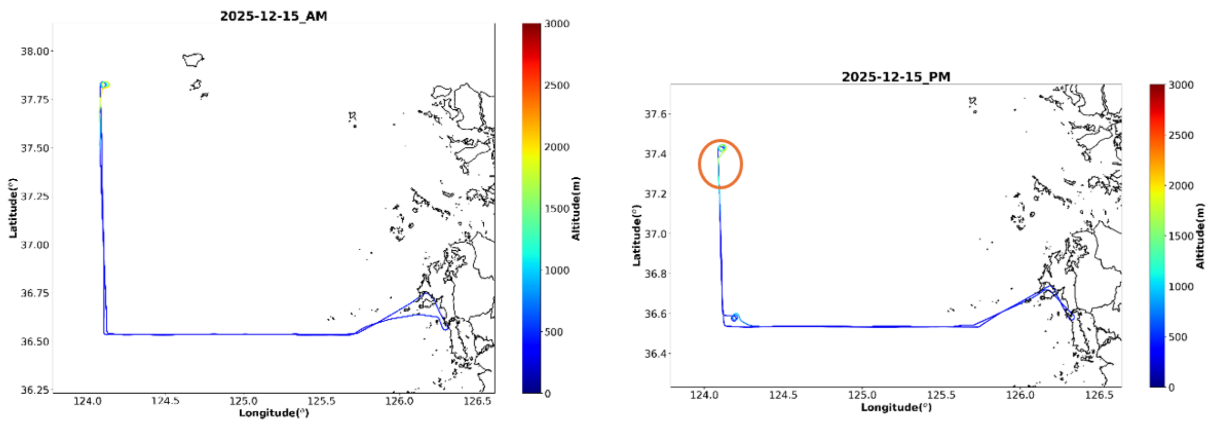

Figure R3. Flight tracks for Dec. 15 AM (left) and Dec. 15 PM (right), color-coded by altitude (m). Both flights followed an identical spatial corridor over the Yellow Sea, departing from and returning to the Anmyeon-do coast. The orange circle in the Dec. 15 PM panel marks the vertical sounding maneuver conducted at approximately 14:50 KST near 37.4°N, 124.1°E, before and after which the horizontal flight path was identical *to the AM flight.*

L263-267: The concurrent rise in CO and CO_2 concentrations from AM to PM on the day, observed along an identical flight corridor (Figure S1), resulted in a slightly increased CO/CO_2 ratio of 0.50±0.20. This gradual enhancement in both aerosol loading and the CO/CO_2 ratio reflects the continuous transport of regional pollutants, indicating the transition from background conditions to an active inflow and aging regime.

4. Line 241-242, the second rBC size mode is not shown.

Upon reconsideration, we acknowledge that a bimodal distribution is not clearly discernible in the rBC core size distribution. Rather than adding a supporting figure, we have revised the manuscript by removing the description of multiple modes from the text and retaining only the mass median diameter (MMD), which is well-supported by Figure 1. We believe this revision better reflects the observed distribution and avoids overstating the spectral features.

5. Since this work uses the time-lag method, the corresponding coating thickness at the 2 μs threshold should be listed. Given that the scattering detection limit is 174.0 nm, while Bin 1 selects rBC particles with core diameters smaller than 140 nm, this criterion may be largely biased. For example, an rBC particle with a core diameter <140 nm and a coating thickness of 15 nm (typically considered thickly coated) would likely be classified as thinly or not coated, since no scattering peak may be detected.

We fully appreciate the concern regarding optical detection limits and the operational *definition of the 2 um time-lag threshold. Below, we clarify the methodological distinctions between the time-lag and Leading Edge Only-fit (LEO-fit) approaches, the physical equivalence of the threshold, and the physical meaning of the optical detection limit in our dataset.*

While the LEO-fit method retrieves absolute coating thickness using Mie theory, it is generally bounded by both a lower scattering detection limit (~170 nm) and an upper core limit (D_{core} ~ 220 nm) due to APD detector saturation. In contrast, the time-lag method tracks the measurable evaporation delay (delta t ~1- 2 us) between scattering and incandescence peaks as non-refractory coatings evaporate first in the laser beam (Lim et al., 2023; Moteki and Kondo, 2007). This enables an operational assessment of internal mixing across broader core sizes without core diameter constraints.

To quantitatively resolve the physical coating thickness corresponding to the 2 us threshold, we directly compared the 2D density distributions of delay time versus core diameter against LEO-fit retrievals from the same airborne dataset. Across the dominant core size range within the robust LEO-fit window (D_{core} = 170-200 nm), the 2 us threshold corresponds to an effective coating thickness of ~20-30 nm. This information is added in the revised manuscript.

The scattering detection limit of ~174 nm is fundamentally defined based on calibration for purely scattering (non-BC) particles. When retrieving the overall optical size of BC-containing particles (e.g., via LEO-fit), restricting calculations to within this robust optical detection range is recommended to ensure numerical precision in optical cross-sections.

However, time-lag analysis does not aim to quantitatively invert the absolute optical diameter. Instead, it relies on identifying the temporal delay between the registered scattering peak and incandescence peak for absorbing rBC cores. In airborne observations, smaller rBC cores frequently constitute a substantial portion of the particle number population. Because *the LEO-fit method is severely truncated at the lower end by optical detection limits (as well as at the upper end by detector saturation), the time-lag derived F_{thick} was preferentially chosen to characterize the mixing state across the entire observed rBC core size spectrum. Consequently, the optical sizing bias raised by the reviewer does not compromise our reported F_{thick} results or overall conclusions.*

L183: Also, within the robust analytical window (core diameter of ~170-200 nm), the 2 μs threshold corresponds to an effective coating thickness of approximately 20–30 nm.

Minor:

1. Page 2 Line 67-72: There is only one reference for each season, and both refer to the same location. The study location should be specified since it may not be validated for other locations.

We thank the reviewer for this constructive comment. We have revised the manuscript to address both concerns. First, the study location has been explicitly specified as urban Seoul for both seasonal observations. Second, to avoid over-reliance on single-location references, we have added supporting literature from East Asia (Kompalli et al., 2020; Liu et al., 2019) that corroborates the seasonal contrast in BC mixing state across the broader region, before narrowing to the Seoul-specific findings. The revised text now reads:

L74-85: In general, while condensation of low volatile and oxygenated gases forms secondary aerosol on BC surfaces, the amount of secondary aerosol coating and its formation rate depend on complex atmospheric chemical and physical state and its interplay with meteorology (Lim et al., 2023, 2025; Peng et al., 2016; Riemer et al., 2010). In East Asia, the mixing state and secondary coating of BC exhibit pronounced seasonality with thicker in winter and thinner coatings in summer (Kompalli et al., 2020; Liu et al., 2019), which is tightly coupled with ambient PM loadings and meteorological conditions. Specifically, observations in urban Seoul demonstrate this sharp contrast. During warm summertime under clean marine influence, the majority of BC particles (>70%) remain bare or thinly coated with daytime coating growth rates of a few nm per hour largely due to limited condensable materials as well as high air temperature, e.g. above 25 °C (Lim et al., 2023). In contrast, during transboundary winter haze periods, BC aerosols were thickly coated, reflecting enhanced secondary aerosol formation under chemically oxidized, high-PM conditions (Lim et al., 2025).

2. Line 71, wrong capital "Temperature"

It has been corrected.

3. Line 202-203, the bimodal distribution cannot be seen from Figure 1. A supporting figure should be added.

Upon reconsideration, we acknowledge that a bimodal distribution is not clearly discernible in the rBC core size distribution. Rather than adding a supporting figure, we have revised the manuscript by removing the description of multiple modes from the text and retaining only the mass median diameter (MMD), which is well-supported by Figure 1. We believe this revision better reflects the observed distribution and avoids overstating the spectral features.

4. Line 204-205, please specify remote background conditions.

We have revised the manuscript to specify the remote background conditions by explicitly referencing the Gosan Climate Observatory at Jeju Island.

L253-256: The mean F_{thick} value (0.62) revealed that the rBC particles remained consistent with remote background levels of Gosan Climate Observatory in Jeju Island (Lim et al., 2022), showing minimal impact from fresh anthropogenic pollution.

5. Line 209 PBLH undefined throughout the context.

We thank the reviewer for this comment. We acknowledge that the acronym PBLH was not defined upon its first use. To address this and to improve clarity throughout the manuscript, we have revised our treatment of boundary layer terminology as follows.

While the marine boundary layer (MBL) is intrinsically shallower than a continental planetary boundary layer (PBL), explicit MBL height data were unavailable over the flight tracks. As a robust alternative, we evaluated the in situ vertical profiles of rBC mass concentration (M_{rBC}) alongside the ECMWF ERA5 PBL height (PBLH) across all research flights to assess the vertical boundary layer structure and verify the heights of the MBL and residual layer (Figure S2). This approach is based on the fact that BC core is a primary pollutant that neither evaporates nor forms via atmospheric chemical reactions. The PBLH was obtained from the ECMWF reanalysis grid point the observation location.

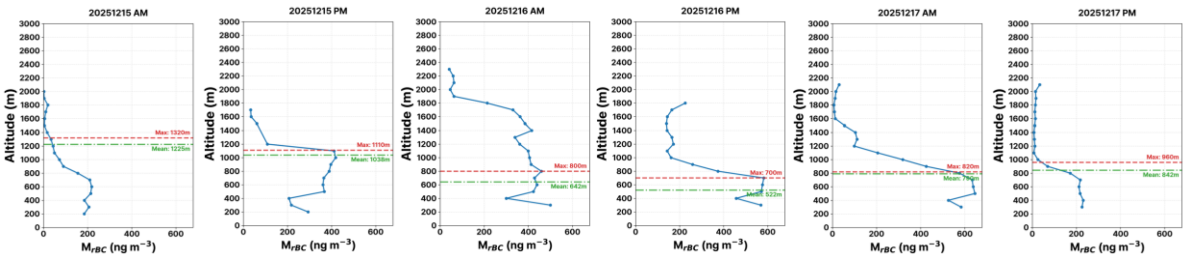

Figure S2. Vertical profiles of M_{rBC} observed during each research flight from 15 to 17 December 2025 over the Yellow Sea. Horizontal dashed lines indicate the *estimated planetary boundary layer height (PBLH) obtained from the ECMWF reanalysis at the grid point nearest to the observation location. Red and green dashed lines denote the maximum and mean PBLH, respectively, with annotated values (in m a.s.l.) shown for each flight.*

Overall, the observed vertical profiles of M_{rBC} show generally good agreement with the estimated PBLH across the flight campaign. During the 15 Dec. flights (both AM and PM), a sharp decrease in M_{rBC} at approximately 1.0-1.2 km a.s.l. aligns closely with the PBLH. Similarly, for the 16 Dec. PM and 17 Dec. flights, the altitudes at which M_{rBC} decreased rapidly are broadly consistent with the PBLH, supporting the use of the M_{rBC} vertical structure as an indicator of boundary layer extent. The most notable exception occurred during the 16 Dec. AM flight, where substantial M_{rBC} loadings persisted up to ~1.8 km while the PBLH was estimated near ~600–800 m. This discrepancy suggests that an elevated aerosol layer, likely associated with continental outflow, existed above the shallow marine boundary layer, consistent with a residual layer structure previously reported in the Yellow Sea region (Lee et al., 2019). Given the close correspondence between the altitude of sharp M_{rBC} decreases and the ERA5-derived PBLH across most research flights (Figure S3), the ERA5 PBLH was adopted as the representative boundary layer height for each flight in subsequent analyses. This comparison is added in Supplementary Information S2.

6. Line 228-229, 1 mm is total precipitation?

We thank the reviewer for this observation. We agree that 1 mm recorded at Incheon represents total precipitation at a coastal land station and may not fully reflect precipitation over the Yellow Sea flight domain. To address this, we have revised as follows.

L278: **Pollution accumulation (RF4, Dec. 16 PM):** After a slight shower (e.g., 1 mm in Incheon, a western coastal city proximal to the flight domain), ...

7. Figure 1, the unit for rBC mass concentration is missing.

The unit for rBC mass concentration (ng m^{-3}) was missing from Figure 1 and has been added to the axis label in the revised manuscript accordingly.

8. Line 302, SIA undefined.

   It has been defined as follows.

L328: Furthermore, the mutual DRH of internally mixed secondary inorganic aerosol (SIA) systems is..

References

Kompalli, S. K., Suresh Babu, S. N., Satheesh, S. K., Krishna Moorthy, K., Das, T., Boopathy, R., Liu, D., Darbyshire, E., Allan, J. D., Brooks, J., Flynn, M. J., and Coe, H.: Seasonal contrast in size distributions and mixing state of black carbon and its association with PM1.0 chemical composition from the eastern coast of India, Atmos. Chem. Phys., 20, 3965–3985, https://doi.org/10.5194/acp-20-3965-2020, 2020.

Lee, H.-J., Jo, H.-Y., Kim, S.-W., Park, M.-S., and Kim, C.-H.: Impacts of atmospheric vertical structures on transboundary aerosol transport from China to South Korea, J. Geophys. Res.-Atmos., 124, 6532–6553, https://doi.org/10.1029/2018JD029751, 2019.

Lim, S., Lee, M., Laj, P., Kim, S.-W., Ahn, K.-H., Gil, J., Shang, X., Zanatta, M., and Kang, K.-S.: Regional characteristics of fine aerosol mass increase elucidated from long-term observations and KORUS-AQ campaign at a Northeast Asian background site, Elementa Sci. Anthrop., 10, 00020, https://doi.org/10.1525/elementa.2022.00020, 2022.

Lim, S., Bae, M.-S., Jang, J., Dwivedi, A. K., Gil, J., Kim, J., Lee, M., Oh, S.-H., Shin, S.-A., and Chang, L.-S.: Exploring fine-aerosol episodes in urban Seoul during the cold season of the 2021 SIJAQ campaign: measurement evidences of heterogeneous reactions on black carbon particles, Atmos. Environ., 342, 120926, https://doi.org/10.1016/j.atmosenv.2024.120926, 2025.

Moteki, N. and Kondo, Y.: Effects of mixing state on black carbon measurements by laser-induced incandescence, Aerosol Sci. Technol., 41, 398–417, https://doi.org/10.1080/02786820701199728, 2007.